SEMARAK ILMU PUBLISHING

Journal of Advanced Research in Applied Sciences and Engineering Technology

Journal homepage:
https://semarakilmu.com.my/journals/index.php/applied_sciences_eng_tech/index
ISSN: 2462-1943

Numerical Investigation of Diffusion thermo and Thermal Diffusion on Mixed Convection flow of Williamson Nanofluid through a vertical cone with porous material in the presence Thermal radiation and Activation Energy

Indira Sundaram[1,*], Srinivasa Raju Rallabandi[2]

[1] Department of Mathematics, CVR College of Engineering, Hyderabad, 501506, Telangana State, India
[2] Department of Mathematics, GITAM (Deemed to be university), Hyderabad campus, Rudraram, Sanga Reddy (Dt), 502329, Telangana State, India

ARTICLE INFO

Article history:
Received 15 September 2023
Received in revised form 27 December 2023
Accepted 11 April 2024
Available online 22 May 2024

Keywords:
Williamson nanofluid; MHD; Diffusion thermo; Thermal Diffusion; Thermal Radiation.

ABSTRACT

In this paper, analyze the impact of Activation energy, Diffusion thermo and thermal diffusion with heat and mass transfer inherent of over a vertical cone through Thermally Radiant Williamson nanofluid with saturated porous medium under the convective boundary condition in the presence of thermal radiation has been studied. The coefficients of Brownian and thermophoresis diffusions are also taken into consideration. The governing partial differential equations are reduced to a couple of nonlinear ordinary differential equations by using suitable transformation equations; these equations are then solved numerically with the use of the conventional fourth-order Runge Kutta method accompanied by the shooting technique. As a result, the effects of various physical parameters on the velocity, temperature, and nanoparticle concentration profiles as well as on the skin friction coefficient and rate of heat transfer are discussed with the aid of graphs and tables. This study has been directly applied in the pharmaceutical industry, microfluidic technology, microbial improved oil recovery, modelling oil and gas-bearing sedimentary basins, and many other fields. Further, to check the accuracy and validation of the present results, satisfactory concurrence is observed with the existing literature.

1. Introduction

Non-Newtonian fluids are extensively implemented in diverse industrial processes such as petroleum drilling, drawing of plastic films, fibre spinning, and food production. The Williamson fluid model is one of the simplest non-Newtonian models to replicate the viscoelastic shear-thinning attributes, see Williamson [1]. The flow of thermally radiative Williamson fluid on a stretching sheet with chemical reaction was disclosed by Krishnamurthy *et al.,* [2]. They proved the fluid temperature falling off due to the presence of the Williamson parameter. Khan *et al.,* [3] demonstrated the impact

[*] *Corresponding author.*
E-mail address: indirakannan75@gmail.com

https://doi.org/10.37934/araset.45.2.90110

of slip flow of Williamson nanofluid in a porous medium. They exposed that the surface drag force suppresses due to rising the Williamson fluid parameter. The 2D unsteady radiative Williamson fluid flow on a permeable stretching surface was deliberated by Hayat *et al.,* [4]. They noticed that the fluid speed becomes slow when the Williamson parameter is high. Nadeem *et al.,* [5] examined the Williamson fluid flow past a stretching sheet, and they found that the skin friction coefficient decreases with enhancing the Williamson parameter. Make use of the Keller box procedure to solve the problem of MHD flow of Williamson fluid over a stretching sheet by Salahuddin *et al.,* [6]. Their outcome shows that the Williamson fluid parameter leads to suppress the fluid velocity. Few significant analysis for this area is seen in Refs. [7].

Heat and mass transfer in non-Newtonian fluid flow through porous medium in engineering has extensive application, such as ventilation procedure, oil production, solar collection, cooling of nuclear reactors, and electronic cooling. Accordingly, Raghunath *et al.,* [8] have studied processing to pass unsteady MHD flow of a second-grade fluid through a porous medium in the presence of radiation absorption exhibits Diffusion thermo, hall and ion slip effects. Raghunath *et al.,* [9] Radiation absorption on MHD Free Conduction flow through porous medium over an unbounded vertical plate with heat source. Li *et al.,* [10] have studied Effects of activation energy and chemical reaction on unsteady MHD dissipative Darcy–Forchheimer squeezed flow of Casson fluid over horizontal channel**.** Suresh Kumar [11] have expressed Numerical analysis of magneto hydrodynamics Casson nanofluid flow with activation energy, Hall current and thermal radiation. Aruna *et al.,* [12] have possessed an unsteady MHD flow of a second-grade fluid passing through a porous medium in the presence of radiation absorption exhibits Hall and ion slip effects. Raghunath *et al.,* [13] have studied Hall current and thermal radiation effects of 3D rotating hybrid nanofluid reactive flow via stretched plate with internal heat absorption. Raghunath *et al.,* [14] have analysed unsteady magneto-hydro-dynamics flow of Jeffrey fluid through porous media with thermal radiation, Hall current and Soret effects. Raghunath [15] has studied Study of Heat and Mass Transfer of an Unsteady Magnetohydrodynamic Nanofluid Flow Past a Vertical Porous Plate in the Presence of Chemical Reaction, Radiation and soret Effects. Raghunath et al., [16] have studied Diffusion Thermo and Chemical Reaction Effects on Magnetohydrodynamic Jeffrey Nanofluid over an Inclined Vertical Plate in the Presence of Radiation Absorption and Constant Heat Source. Maatoug et al., [17] have discussed Variable chemical species and thermo-diffusion Darcy–Forchheimer squeezed flow of Jeffrey nanofluid in horizontal channel with viscous dissipation effects. Bafakeeh et al., [18] have analysed Hall current and Soret effects on unsteady MHD rotating flow of second-grade fluid through porous media under the influences of thermal radiation and chemical reactions. Deepthi et al., [19] have possessed recent development of heat and mass transport in the presence of Hall, ion slip and thermo diffusion in radiative second grade material: application of micromachines.

When heat and mass transfer occurs simultaneously in a moving fluid, the energy flux caused by a concentration gradient is termed as diffusion thermo effect, whereas mass fluxes can also be created by temperature gradients which is known as a thermal diffusion effect. These effects are studied as second-order phenomena and may have significant applications in areas like petrology, hydrology, and geosciences. Raghunath *et al.,* [22] has analyzed Diffusion Thermo and Chemical Reaction Effects on Magnetohydrodynamic Jeffrey Nanofluid over an Inclined Vertical Plate in the Presence of Radiation Absorption and Constant Heat Source. Maatoug *et al.,* [23] have expressed Variable chemical species and thermo-diffusion Darcy–Forchheimer squeezed flow of Jeffrey nanofluid in horizontal channel with viscous dissipation effects. Omar *et al.,* [24] have possessed Hall Current and Soret Effects on Unsteady MHD Rotating Flow of Second-Grade Fluid through Porous Media under the Influences of Thermal Radiation and Chemical Reactions. Deepthi *et al.,* [25] have discussed Recent Development of Heat and Mass Transport in the Presence of Hall, Ion Slip and

Thermo Diffusion in Radiative Second Grade Material: Application of Micromachines. Rani and Kim [20] studied numerically the laminar flow of an incompressible viscous fluid past an isothermal vertical cylinder with Soret and Dufour effects. The effects of chemical reaction and Soret and Dufour on the mixed convection heat and mass transfer of viscous fluid over a stretching surface in the presence of thermal radiation were analyzed by Pal and Mondal [21]. Sharma *et al.,* [22] studied the mixed convective flow, heat and mass transfer of viscous fluid in a porous medium past a radiative vertical plate with chemical reaction, and Soret and Dufour effects.

Activation energy is the smallest amount of energy needed by chemical reactants to endure a chemical reaction. The influence of activation energy on convective heat and mass transfer in the region of boundary layers was initially inspected by Bestman [23]. Later, many researchers have studied the impact of activation energy on heat and mass transfer of boundary layer flow of the fluids. Among those researchers, Awad *et al.,* [24], Dhlamini *et al.,* [25], Anuradha and Sasikala [26], and Hamid *et al.,* [27] scrutinized the influence of activation energy on heat and mass transfer in unsteady fluid flow under different geometry. Moreover, Huang [28] and Mustafa [29] studied the effect of activation energy on MHD boundary layer flow of nanofluids past a vertical surface and permeable horizontal cylinder. Further investigations on the effect of activation energy on non-Newtonian fluid under different surfaces are stated in [30–33]. From their plots, it can be seen that as the values of the activation energy parameter upsurges, the concentration nanoparticles increase.

The aforementioned studies and open literature survey bear witness effects of Activation energy, Diffusion thermo and Thermal Diffusion on two-dimensional laminar and incompressible steady flow of thermally radiant Williamson nanofluid through vertical cone with porous material in the presence of thermal radiation has been presented. The highly non-linear partial differential equations are simplified by using suitable similarity transformation equations and the reduced equations are solved numerically with the help of the conventional fourth-order Runge Kutta method along with the shooting procedure. Discussion on the results is deliberated through graphs and tables for some pertinent parameters of interest. Moreover, a comparison of the numerical results was checked and the validity of the method with published works was made; it shows nice agreement.

2. Flow Governing Equations

The steady, laminar, and incompressible flow of Williamson fluid over stretching surface considered as cone with porous material. The boundary surface of geometries is imposed with convective conditions. Brownian motion and thermophoresis influences are also considered. The stretching velocity of the surface is taken as $u_w = x\upsilon/L^2$, whereas the suction/injection velocity is taken as v_w. The surface temperature is taken as $T_w = T_\infty + ax^{r1}$, where a and r_1 represent the constant and wall thermal factor, respectively. The concentration near the surface is taken as $C_w = C_\infty + ax^{r2}$, where r_2 represents the nanofluid concentration parameter. The half angle of the cone is taken by α, with radius r. The physical model of the geometry is shown in Figure 1.

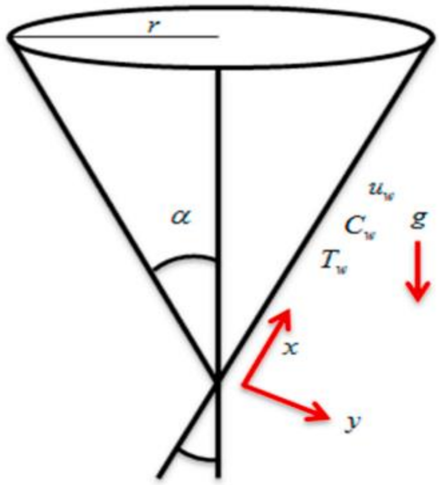

Fig. 1. Physical configuration of the problem

By considering the works of Raghunath *et al.,* [34] and by employing the Boussinesq approximation the governing equations describing steady-state conservation of mass, momentum, energy as well as conservation of nanoparticles for nanofluids in the presence of thermal radiation, activation energy and other important take the following form:

$$\frac{\partial}{\partial x}(ru)+\frac{\partial}{\partial y}(rv)=0 \tag{1}$$

$$u\frac{\partial u}{\partial x}+v\frac{\partial u}{\partial y}=\upsilon\frac{\partial^2 u}{\partial x^2}-\sqrt{2}\upsilon\Gamma\frac{\partial u}{\partial y}\frac{\partial^2 u}{\partial y^2}+ \\ g\left[(1-C_\infty)_{\rho f_\infty}\beta(T-T_\infty)-\left(\rho_p-\rho_{f_\infty}\right)(C-C_\infty)\right]Cos\gamma \tag{2}$$

$$u\frac{\partial T}{\partial x}+v\frac{\partial T}{\partial y}=\alpha\frac{\partial^2 T}{\partial y^2}+\tau\left(D_B\frac{\partial T}{\partial y}\frac{\partial C}{\partial y}+\frac{D_T}{T_\infty}\left(\frac{\partial T}{\partial y}\right)^2\right)-\frac{1}{\rho C_p}\frac{\partial q_r}{\partial y}+\frac{D_m k_T}{c_s c_p}\frac{\partial^2 C}{\partial y^2} \tag{3}$$

$$u\frac{\partial C}{\partial x}+v\frac{\partial C}{\partial y}=\frac{D_m k_T}{T_m}\frac{\partial T^2}{\partial y^2}+D_B\frac{\partial^2 C}{\partial y^2}+\left(\frac{D_T}{T_\infty}\right)\frac{\partial T^2}{\partial y^2}-k^2{}_r\left(\frac{T}{T_\infty}\right)e^{(-E_{a/kT})}(C-C_\infty) \tag{4}$$

For this flow, corresponding boundary conditions are

$$u=u_w, v=-v_w, -k^*\frac{\partial T}{\partial y}=h_1(T_w-T),\ D_B\frac{\partial T}{\partial y}+\frac{D_T}{T_\infty}\frac{\partial T}{\partial y}=0\ at\ \ y=0 \\ u\to 0,\ T\to T_\infty,\ C\to C_\infty\ as\ y\to\infty \tag{5}$$

where u and v are the velocity components in their respective directions, β_T is the coefficient of volumetric thermal expansion, β_C is the volumetric concentration expansion, υ is the kinematic viscosity, ρ is the density, L is the characteristics length, τ is the extra stress tensor, Γ is the positive time constant, D_B and D_T are the diffusion coefficients of Brownian and thermophoresis, respectively, αis the thermal conductivity, T is the temperature, C is the concentration. E is the nondimensional activation energy, δ is the temperature difference parameter. The subscripts w and ∞ represent conditions near the wall and ambient from the wall, respectively.

The radiative heat flux q_r (using Roseland approximation followed [24]) is defined as

$$q_r = -\frac{4\sigma^*}{3K^*}\left(\frac{\partial T^4}{\partial y}\right) \tag{6}$$

We assume that the temperature variances inside the flow are such that the term T^4 can be represented as linear function of temperature. This is accomplished by expanding T^4 in a Taylor series about a free stream temperature T_∞ as follows:

$$T^4 = T_\infty^4 + 4T_\infty^3\left(T - T_\infty\right) + 6T_\infty^2\left(T - T_\infty\right)^2 + \ldots\ldots\ldots\ldots \tag{7}$$

After neglecting higher-order terms in the above equation beyond the first degree term in $\left(T - T_\infty\right)$, we get

$$T^4 \cong 4T_\infty^3 T - 3T_\infty^4 \tag{8}$$

Thus substituting Eq. (8) in Eq. (6), we get

$$q_r = -\frac{16T_\infty^3\sigma^*}{3K^*}\left(\frac{\partial T}{\partial y}\right) \tag{9}$$

Using (9), Eq. (3) can be written as

$$u\frac{\partial T}{\partial x} + v\frac{\partial T}{\partial y} = \alpha\frac{\partial^2 T}{\partial y^2} + \tau\left(D_B\frac{\partial C}{\partial y}\frac{\partial T}{\partial y} + \frac{D_T}{T_\infty}\left(\frac{\partial T}{\partial y}\right)^2\right) + \frac{1}{\rho C_p}\frac{16T_\infty^3\sigma^*}{\partial K^*}\left(\frac{\partial^2 T}{\partial y^2}\right) + \frac{D_m k_T}{c_s c_p}\frac{\partial^2 C}{\partial y^2} \tag{10}$$

The following similarity variables are introduced for solving governing equations (2), (6) and (4) as

$$\eta = \frac{y}{L}, u = \frac{xD}{L}f'(\eta), v = \frac{\upsilon(1+m)}{L}f(\eta), \ \theta(\eta) = \frac{T - T_\infty}{T_w - T_\infty}, \ \phi(\eta) = \frac{C - C_\infty}{C_w - C_\infty} \tag{11}$$

Substituting Eq. (11) into Eqs. (2), (3) and (4), we get the following system of non-linear ordinary differential equations

$$f''' + Wf''f''' + (1+m)ff'' - f'^2 + Gr\theta Cos\alpha + Gc\phi Cos\alpha - Mf' = 0 \tag{12}$$

$$\theta''(1+R_d)+\Pr\left[(1+m)f\theta'-r_1 f'\theta+\left(N_b\,\theta'\,\phi'+N_t\theta'^2\right)+D_u\,\phi'\right]=0 \tag{13}$$

$$\phi''+Sc\left[(1+m)f\phi'-r_2 f'\phi-\sigma[1+\delta\theta]^n\exp\left[\frac{-E}{1+\delta\theta}\right]\phi\right]+\left(S_r L_e+\frac{N_t}{N_b}\right)\theta''=0 \tag{14}$$

The corresponding boundary conditions (5) become

$$\begin{aligned} &f(0)=S,\quad f'(0)=1,\ f'(\infty)=0,\theta'(0)=B_i(\theta(0)-1),\\ &\theta(\infty)=0,\ \phi'(0)=-\frac{Nt}{Nb}\theta'(0),\ \phi(\infty)=0. \end{aligned} \tag{15}$$

where prime denotes differentiation with respect to η, and the significant thermophysical parameters indicating the flow dynamics are defined by

$W=\frac{\sqrt{2}\Gamma u_w}{L}$ is the Williamson parameter,

$\Pr=\frac{\alpha}{\mu C_p}$ is the Prandtl number,

$N_b=\frac{\tau D_B(C_w-C_\infty)}{\upsilon}$ is the Brownian motion parameter,

$N_t=\frac{\tau D_T(T_w-T_\infty)}{\upsilon T_\infty}$ is the thermophoresis parameter,

$B_i=\frac{Lh_1}{k}$ is the Biot number,

$E=\frac{E_a}{kT_\infty}$ is the non-dimensional activation energy,

$\delta=\frac{(T_w-T_\infty)}{T_\infty}$ Is the temperature difference parameter,

$\sigma=\frac{k_r^2}{a}$ is the non-dimensional reaction rate,

$Gr=\frac{gL^2\beta_T(T_w-T_\infty)}{\upsilon u_w}$ Is the thermal Grashof number,

$Gc=\frac{gL^2\beta_T(C_w-C_\infty)}{\upsilon u_w}$ is the concentration Grashof number,

$R_d=\frac{14\sigma^* T_\infty^3}{3kK^*}$ is the thermal Radiation parameter,

$Du=\frac{D_M k_T(C_w-C_\infty)}{C_S C_p \upsilon\alpha^2(T_w-T_\infty)}$ is the Diffusion thermo parameter,

$S_r=\frac{D_m k_T(T_w-T_\infty)}{T_m\alpha_m(C_w-C_\infty)}$ is the Thermal Diffusion parameter.

The quantities we are interested to study are the skin friction coefficient C_f , the local Nusselt number N_{ux} and the local Sherwood number S_{hx}. The quantities are defined as:

$$C_f = \frac{\tau_w}{\rho u_w^2} = \frac{\mu\left[\frac{\partial u}{\partial y} + \frac{\Gamma}{\sqrt{2}}\left(\frac{\partial u}{\partial y}\right)^2\right]_{y=0}}{\rho\left(\frac{x\upsilon}{L^2}\right)} = f''(0) + \frac{W}{2} f''^2(0) \tag{16}$$

$$Nu_x = \frac{xq_w}{k(T_w - T_\infty)} = \frac{-x\left(\frac{\partial T}{\partial y}\right)_{y=0}}{k(T_w - T_\infty)} = -\theta'(0), \tag{17}$$

$$Sh_x = \frac{x\,j_w}{D_B(C_w - C_\infty)} = \frac{-x\left(\frac{\partial C}{\partial y}\right)_{y=o}}{D_B(C_w - C_\infty)} = -\phi'(0). \tag{18}$$

3. Numerical solution

As Eqs. (12)–(14) are strongly non-linear, it is difficult or maybe impossible to find the closed form solutions. Accordingly, these boundary value problems are solved numerically by using the conventional fourth-order RK integration scheme along with the shooting technique. The first task to carry out the computation is to convert the boundary value problem to an initial value problem.

The first task to carry out the computation is to convert the boundary value problem to an initial value problem.

Let by using the following notations:

$$f = y_1,\ f' = y_2,\ f'' = y_3,\ f''' = y_3',\quad \theta = y_4,\ \theta' = y_5, \theta'' = y_5',\ \phi = y_6,\ \phi' = y_7, \phi'' = y_7'. \tag{19}$$

By using the above variables, the system of first-order ODEs is

$$y_1' = y_2, \tag{20}$$

$$y_2' = y_3, \tag{21}$$

$$y_3' = \frac{1}{1+y_3W}\left(y_2^2 - (1+m)y_1y_3 - Gr\,Cos\alpha\ y_4 - Gc\,Cos\alpha\ y_6 + Ky_2\right), \tag{22}$$

$$y_4' = y_5, \tag{23}$$

$$y_5' = \frac{1}{1+R_d}\left(-\Pr(1+m)y_1y_5 + r_1y_2y_4 - \Pr N_b\left(y_5y_7 + \frac{Nt}{Nb}(y_5)^2\right) - \Pr\ Du\,y_7\right), \tag{24}$$

$$y_6' = y_7, \tag{25}$$

$$y_7' = -S_c(1+m)y_1y_7 + S_cr_2y_2 + S_c\sigma[1+\delta y_4]^n \exp\left[\frac{-E}{1+\delta y_4}\right]y_6 - \left(S_rL_e + \frac{N_b}{N_t}\right)y_5' \tag{26}$$

4. Code Validation

We checked the accuracy of current outcomes with previous literature in the limited case and obtained a fantastic agreement. Table 3 displays a comparison of numeric outcome for Sherwood values of the Diffusion thermo parameter with the published result of Raghunath *et al.,* [34] with an outstanding agreement.

5. Results and Discussion

The set of nonlinear equations with appropriate boundary conditions are solved numerically by Runge Kutta method along with the shooting procedure. To analyze the variation in velocity, thermal, and concentration distributions, Figures 2–6 are displayed. Also, the skin friction factor, Nusselt number, and Sherwood number are displayed through Tables 2 and 3. For the present analysis, the values of fixed parameters are taken as Pr = 1.0, Rd=0.5, Sc = 0.5, K=1.5, r_1 = 1.0, r_2 = 1.0, S = 1.0, Gr = 0.5, E=0.5, δ=0.2, γ = 0.6, Gc = 0.5, Nb = 0.2, Nt = 0.3, W = 1.0, Du=1.0, Sr=1.5 and α = 45^0.

In Figures 2-3 the effects of the thermal Grashof Gr and mass Grashof Gc numbers on the resultant velocity are displayed. As the Grashof number is a ratio of the buoyancy force to the viscous force and it appears due to the natural convection flow, so an increase in the tangential velocity as well as the transverse velocity of the fluid. It happens because of the fact that higher the Grashof number implies higher the buoyancy force which means higher the movement of the flow.

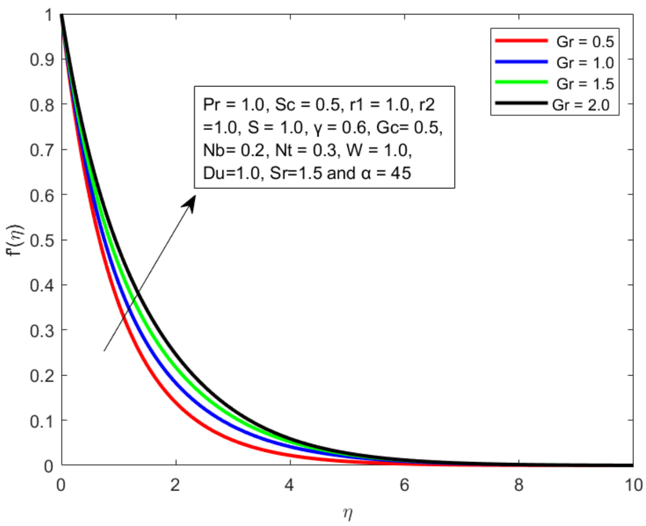

Fig. 2. Effect of Gr on velocity profile

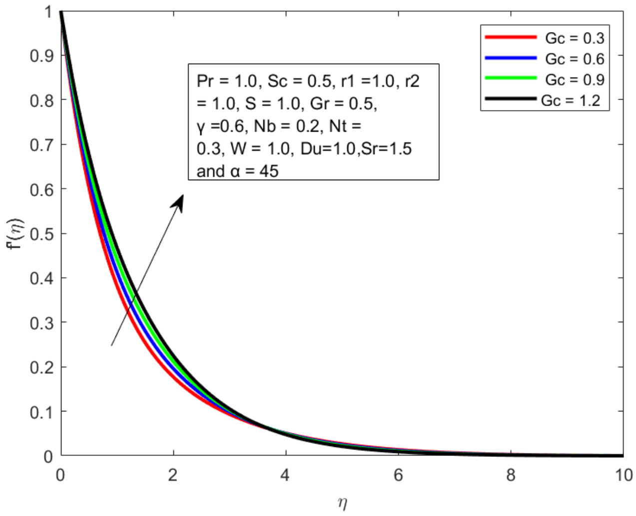

Fig. 3. Effect of Gc on velocity profile

Figures 4-7 depict the influence of the thermal and solutal Grashof number on the temperature and the concentration profile respectively. An increase in the both thermal and solutal Grashof number means a decrease in the viscous force which reduces the temperature and the concentration of the fluid.

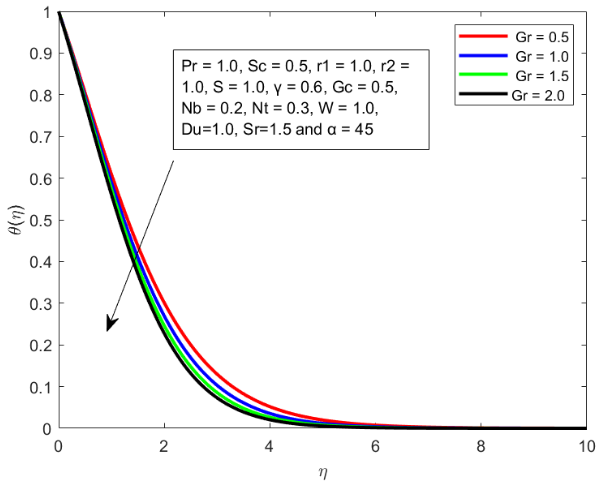

Fig. 4. Effect of Gr on temperature profile

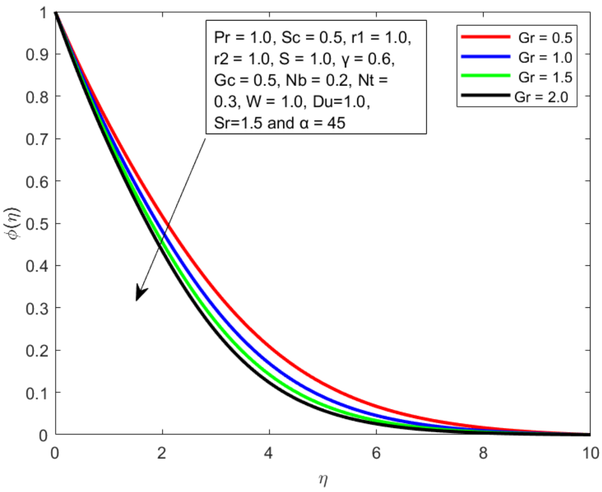

Fig. 5. Effect of Gr on concentration profile

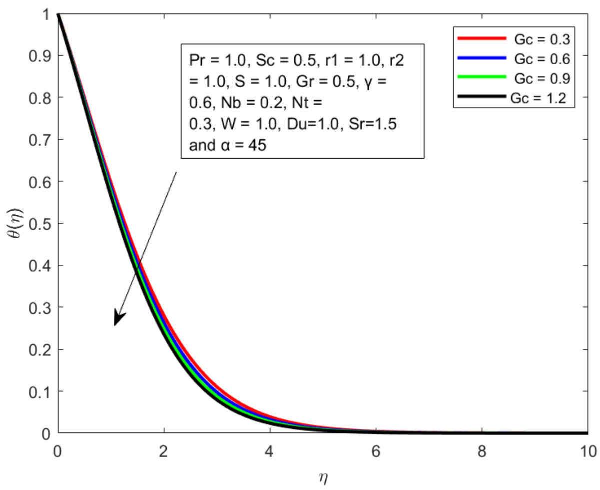

Fig. 6. Effect of Gc on temperature profile

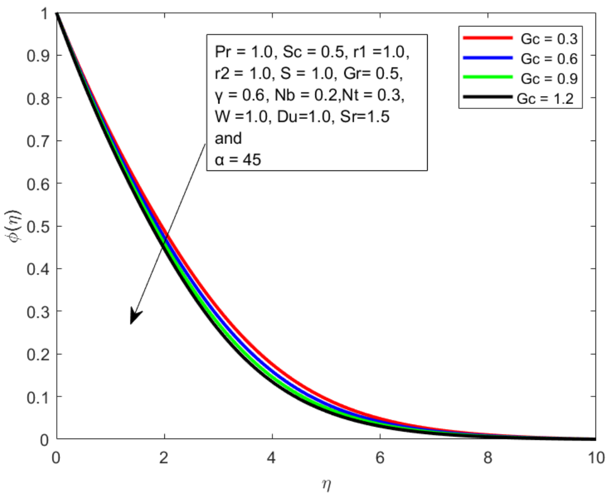

Fig. 7. Effect of Gc on concentration profile

Figures 8-10 shows the impact of the Williamson parameter on velocity, temperature, and concentration distributions. Here, the reducing impact on velocity distribution is perceived with a higher Williamson parameter, while a reducing impression on thermal and concentration distributions is depicted for both geometries. Physically, the increasing Williamson parameter suggests more retardation time for the nanofluid flow particles to regain their original position, increasing the fluid viscosity and, consequently, reducing the velocity distribution. Also, the greater values of the Williamson factor provide more resistance to the nanofluid flow, which concludes enhancement in thermal and concentration of the nanofluid flow.

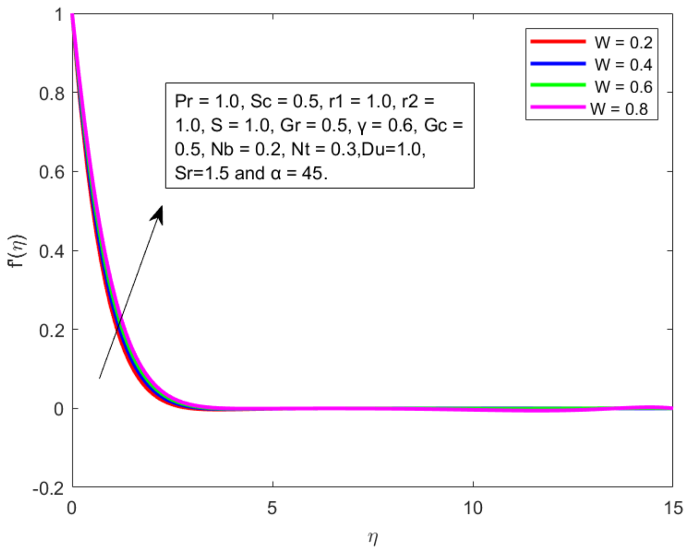

Fig. 8. Effect of W on velocity profile

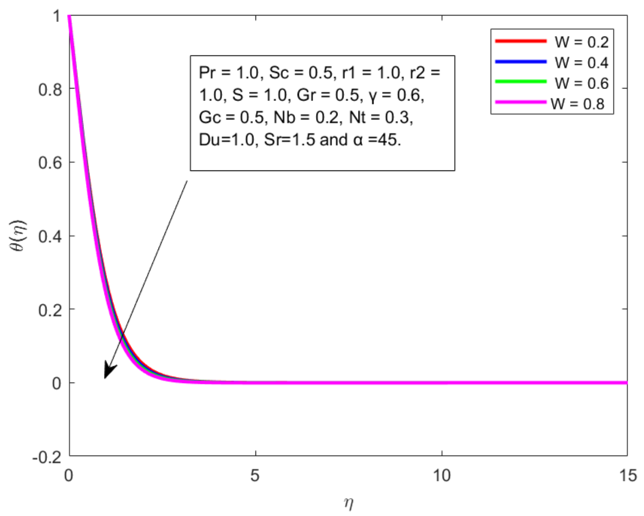

Fig. 9. Effect of W on temperature profile

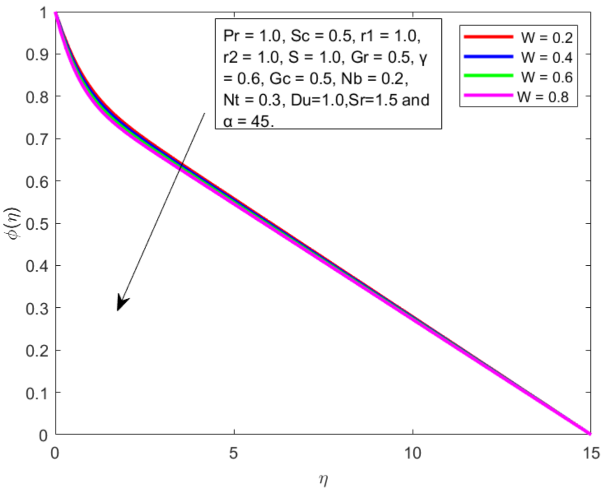

Fig. 10. Effect of W on concentration profile

The temperature and concentration profiles for different values of Brownian motion parameter (Nb) is summarized in Figures 11 and 12. It is investigated that an increases in (Nb), the temperature is extends as shown in Figure 11, whereas the concentration profiles depreciates in Figure 12. This is because of the Brownian motion is the random motion of suspended nanoparticles in the base fluid and is more influenced by its fast moving atoms or molecules in the base fluid. It is mentioned that Brownian motion is related to the size of nanoparticles and are often in the form of agglomerates. Clearly, it can be concluded that Brownian motion parameter has significant influence on the both temperature and concentration.

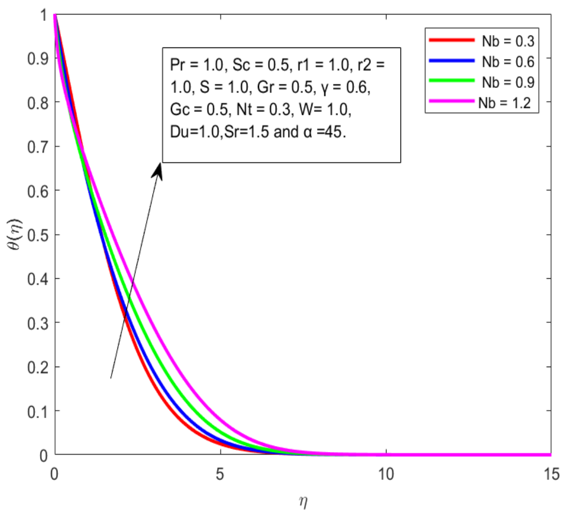

Fig. 11. Effect of Nb on temperature profile

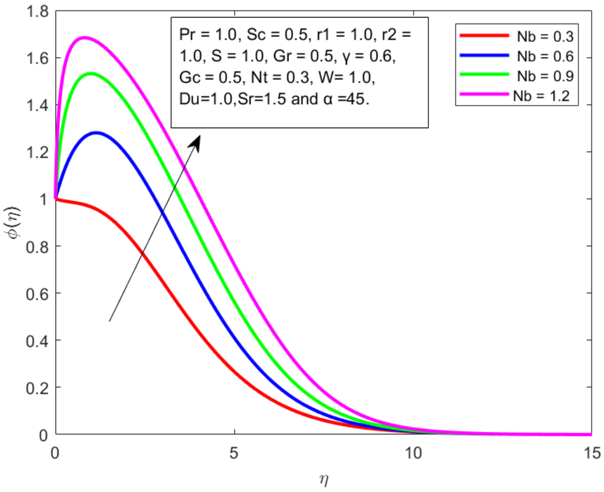

Fig. 12. Effect of Nb on concentration profile

The Variation of non-dimensional temperature and concentration distributions for different values of thermophoretic parameter (Nt) is depicted in Figures 13 and 14. It is noticed from these Figures 13 and 14 that both temperature and concentration profiles boosted in the boundary layer region for the accrual values of thermophoretic parameter (Nt). This is because of the fact that as the values of (Nt) increases the hydrodynamic boundary layer thickness is reduced. This is from the reality that particles near the hot surface create thermophoretic force; this force enhances the temperature and concentration of the fluid in the fluid region.

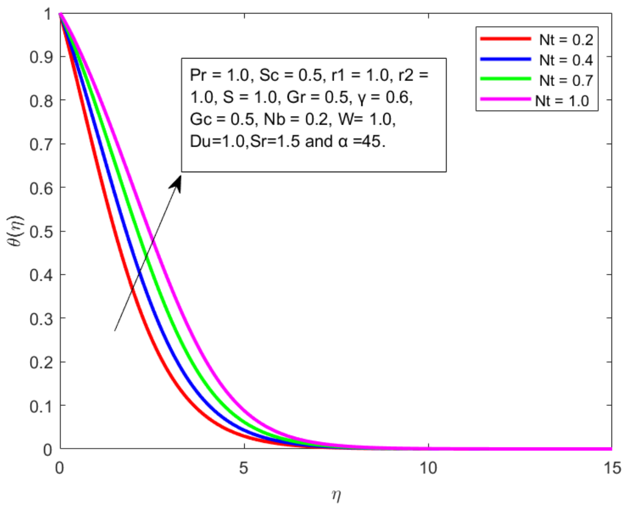

Fig. 13. Effect of Nt on temperature profile

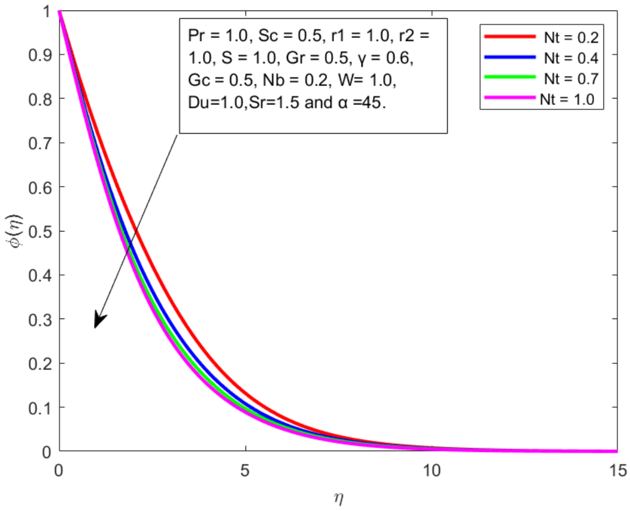

Fig. 14. Effect of Nt on concentration profile

Figure 15 depicts the temperature for the contribution of Diffusion thermo parameter Du. Temperature enhancement is noticed for higher Du values. The same behavior has observed in Figure 16 whereas enhance the concentration profile with increases of thermal diffusion parameter Sr.

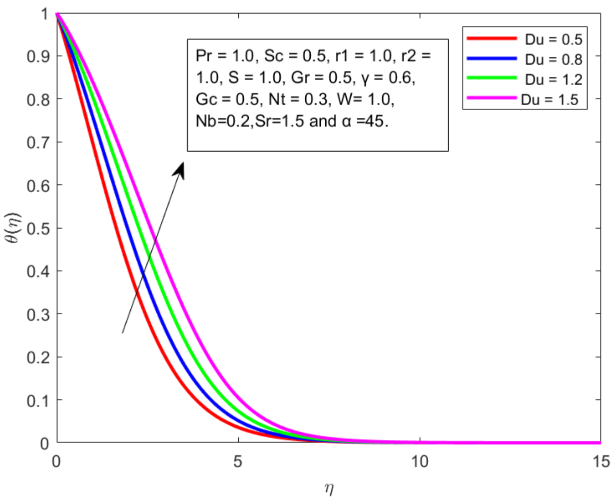

Fig. 15. Effect of Du on temperature profile

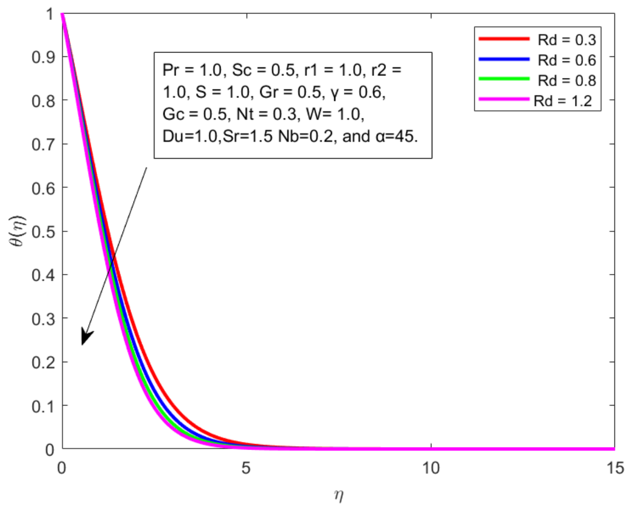

Fig. 16. Effect of Rd on temperature profile

The effect of thermal radiation parameter (Rd) on temperature profile is shown in Figure 17. It is acknowledged that, the thermal boundary layer thickness is enlarged with improving values of radiation parameter (Rd) in the entire boundary layer region of fluid. This is due to the fact that imposing thermal radiation into the flow warmer the fluid, which causes an increment in the temperature.

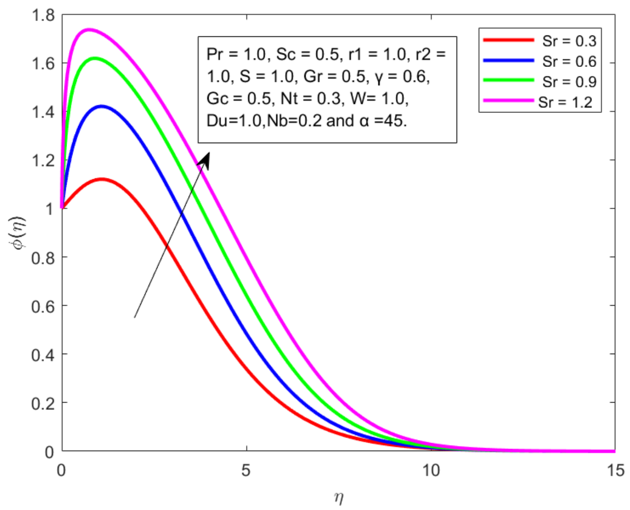

Fig. 17. Effect of Sr on concentration profile

Figure 18 is drawn to show the effects of dimensionless activation energy E on concentration distribution. From the figure, it is revealed that E is dwindling function of increasing values of E with low temperature results in smaller reaction rate constant and eventually slow chemical reaction is observed. This increases the concentration's solute. Figures 19 shows the effect of the chemical reaction rate δ on the solute concentration. It can be observed that an increase in either results in diminishes of concentration profiles as we had shown in Figures 19. This is due to the fact that an increase in either results in an increase in the factor of $[1+\delta\theta]^n \exp\left[\frac{-E}{1+\delta\theta}\right]$ and this results in the favor of destructive chemical reaction due to which concentration decreases.

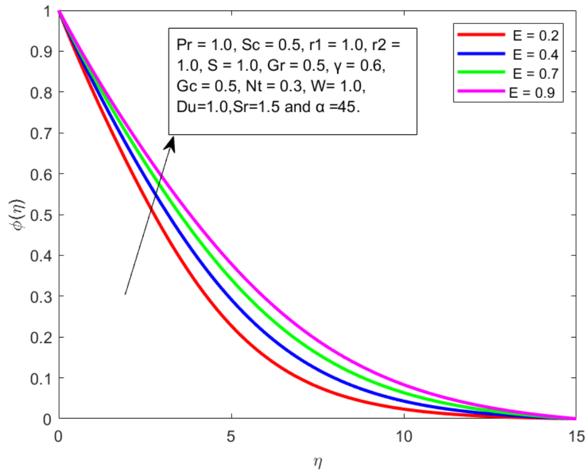

Fig. 18. Effect of E on concentration profile

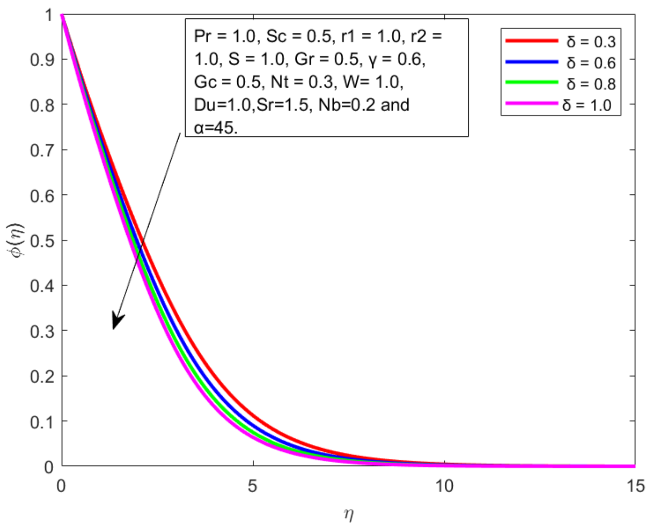

Fig. 19. Effect of δ on concentration profile

The numerical values of C_f for dissimilar values of embedded parameters through cone is displayed in Table 1. From the tabular values, it is concluded that the higher thermal Grashof number increase the skin friction for cone and wedge, while the greater values of solutal Grashof number, wall suction parameter, and Williamson parameter reduces the skin friction. The numerical values of Nu and Sh for different values of embedded factors is displayed in Table 2. From the tabular values, it is concluded that the higher Brownian motion and Diffusion thermo parameters increases the Nusselt number, while reduces the Sherwood number. Higher thermophoresis parameter and thermal radiation diminishes the Nusselt and Sherwood numbers, whereas the reversal behavior has observed in the case of activation energy. To verify the validity and accuracy of the present analysis, the Sherwood number the results for the mass transfer were compared with those reported by Raghunath *et al.,* [34]. The comparison in the above cases is found to be in excellent agreement, as shown in Table 3.

Table 1
Numerical values of C_f for different values of embedded factors through cone and wedge by taking $\alpha = 45^0$

Gr	Gc	S	W	C_f
0.5				−4.6465
1.0				−4.4986
1.5				−4.1431
	0.3			−4.5098
	0.6			−4.7563
	0.9			−5.0098
		0.2		−4.5751
		0.4		−4.8095
		0.6		−5.0763
			0.2	−4.7123
			0.4	−4.9076

Table 2
Numerical values N_u and S_h for different values of embedded factors through cone by taking $\alpha=45^0$

W	K	Rd	E	Nt	Nb	Du	Sr	Nu_z	Sh_z
1.0	1.5	0.5	0.5	0.3	0.2	1.0	1.5	1.9873	0.7575
0.2								1.5464	0.7985
0.4								1.4527	0.6537
	1.0							1.0544	0.7464
	1.5							0.8855	0.9823
		0.3						0.9835	0.8728
		0.6						0.9421	0.7547
			0.2					0.8765	0.7286
			0.4					0.9875	0.9821
				0.3				1.3457	0.9878
				0.4				1.2978	0.8836
					0.3			1.1575	0.9282
					0.6			1.4173	0.7282
						0.5		0.77652	0.42382
						0.8		0.7292	0.4282
							0.3	0.8927	0.8282
							0.6	0.9826	0.6282

Table 3
Comparison of present Sherwood number with the published Sherwood number results of Raghunath *et al.,* [34] when $E=\delta=S=W=r_1=r_2=Gr=Gc=0$

Du	S_h Raghunath *et al.,* [34]	S_h Present values
0.2	0.47452142	0.4787646
0.4	0.44521478	0.4458363
0.6	0.42852147	0.4704746

6. Conclusion

The following is a condensed version of the conclusions that may be drawn from the numerical results:

i. The reducing impact of Williamson parameter on velocity distribution is higher, whereas the opposite behaviors in thermal and concentration distributions are found.
ii. While an increasing conduct is witnessed in the velocity of the nanofluid flow via thermal and solutal Grashof numbers.
iii. An increase in thermal radiation parameter results in an increase in temperature field.
iv. With increasing values of (Nb) temperature profiles optimized, whereas, concentration profiles declines in the entire fluid regime.
v. Both resultant temperature and concentration profiles are enhances with increases Du and Sr values.

Nomenclature

U and v	Velocity components
υ	Kinematic viscosity
ρ	Density
β_T	Coefficient of volumetric thermal expansion
β_c	Coefficient of volumetric concentration expansion
T	Temperature
C	Concentration
f	Nanofluid
D_B	Brownian diffusion coefficient
D_T	Thermophoresis diffusion coefficient
L	Characteristics length
Γ	Positive time constant
W	Williamson parameter
Nb	Brownian motion
Nt	Thermophoresis parameter
γ	Biot number
Gr	Thermal Grashof number
Gc	Concentration Grashof number
Du	Diffusion thermo parameter
Dr	Thermal Diffusion parameter
Rd	Thermal Radiation
E	Activation energy
δ	Rate of chemical reaction
Cf	Skin friction coefficient
Nu	Nusselt number
Sh	Sherwood number
Pr	Prandtl number

Subscripts

w	Condition at the wall
τ	Extra stress tensor

A Thermal conductivity
∞ Condition at the free stream

References

[1] Williamson, R. Vo. "The flow of pseudoplastic materials." *Industrial & Engineering Chemistry* 21, no. 11 (1929): 1108-1111. https://doi.org/10.1021/ie50239a035

[2] Krishnamurthy, M. R., B. C. Prasannakumara, B. J. Gireesha, and Rama Subba Reddy Gorla. "Effect of chemical reaction on MHD boundary layer flow and melting heat transfer of Williamson nanofluid in porous medium." *Engineering Science and Technology, an International Journal* 19, no. 1 (2016): 53-61 https://doi.org/10.1016/j.jestch.2015.06.010.

[3] Khan, M. Ijaz, Faris Alzahrani, Aatef Hobiny, and Zulfiqar Ali. "Modeling of Cattaneo-Christov double diffusions (CCDD) in Williamson nanomaterial slip flow subject to porous medium." *Journal of Materials Research and Technology* 9, no. 3 (2020): 6172-6177. https://doi.org/10.1016/j.jmrt.2020.04.019

[4] Hayat, T., Anum Shafiq, and A. Alsaedi. "Hydromagnetic boundary layer flow of Williamson fluid in the presence of thermal radiation and Ohmic dissipation." *Alexandria Engineering Journal* 55, no. 3 (2016): 2229-2240. https://doi.org/10.1016/j.aej.2016.06.004

[5] Nadeem, S., S. T. Hussain, and Changhoon Lee. "Flow of a Williamson fluid over a stretching sheet." *Brazilian journal of chemical engineering* 30 (2013): 619-625. https://doi.org/10.1590/S0104-66322013000300019

[6] Salahuddin, T., Md Yousaf Malik, Arif Hussain, S. Bilal, and M. Awais. "MHD flow of Cattanneo–Christov heat flux model for Williamson fluid over a stretching sheet with variable thickness: Using numerical approach." *Journal of magnetism and magnetic materials* 401 (2016): 991-997. https://doi.org/10.1016/j.jmmm.2015.11.022

[7] Khan, Najeeb Alam, and Hassam Khan. "A boundary layer flows of non-Newtonian Williamson fluid." *Nonlinear Engineering* 3, no. 2 (2014): 107-115. https://doi.org/10.1515/nleng-2014-0002

[8] Raghunath, Kodi, Ravuri Mohana Ramana, Charankumar Ganteda, Prem Kumar Chaurasiya, Damodar Tiwari, Rajan Kumar, Dharam Buddhi, and Kuldeep Kumar Saxena. "Processing to pass unsteady MHD flow of a second-grade fluid through a porous medium in the presence of radiation absorption exhibits Diffusion thermo, hall and ion slip effects." *Advances in Materials and Processing Technologies* (2023): 1-18. https://doi.org/10.1080/2374068X.2023.2191450

[9] Raghunath, Kodi, Mopuri Obulesu, and Konduru Venkateswara Raju. "Radiation absorption on MHD free conduction flow through porous medium over an unbounded vertical plate with heat source." *International Journal of Ambient Energy* (2023): 1-9. https://doi.org/10.1080/01430750.2023.2181869

[10] Li, Shuguang, Kodi Raghunath, Ayman Alfaleh, Farhan Ali, A. Zaib, M. Ijaz Khan, Sayed M. ElDin, and V. Puneeth. "Effects of activation energy and chemical reaction on unsteady MHD dissipative Darcy–Forchheimer squeezed flow of Casson fluid over horizontal channel." *Scientific Reports* 13, no. 1 (2023): 2666. https://doi.org/10.1038/s41598-023-29702-w

[11] Suresh Kumar, Y., Shaik Hussain, K. Raghunath, Farhan Ali, Kamel Guedri, Sayed M. Eldin, and M. Ijaz Khan. "Numerical analysis of magnetohydrodynamics Casson nanofluid flow with activation energy, Hall current and thermal radiation." *Scientific Reports* 13, no. 1 (2023): 4021. https://doi.org/10.1038/s41598-023-28379-5

[12] Ganjikunta, Aruna, Hari Babu Kommaddi, Venkateswarlu Bhajanthri, and Raghunath Kodi. "An unsteady MHD flow of a second-grade fluid passing through a porous medium in the presence of radiation absorption exhibits Hall and ion slip effects." *Heat Transfer* 52, no. 1 (2023): 780-806.

[13] Kodi, Raghunath, Mohana Ramana Ravuri, V. Veeranna, M. Ijaz Khan, Sherzod Abdullaev, and Nissren Tamam. "Hall current and thermal radiation effects of 3D rotating hybrid nanofluid reactive flow via stretched plate with internal heat absorption." *Results in Physics* 53 (2023): 106915. https://doi.org/10.1016/j.rinp.2023.106915

[14] Kodi, Raghunath, Ramachandra Reddy Vaddemani, M. Ijaz Khan, Sherzod Shukhratovich Abdullaev, Attia Boudjemline, Mohamed Boujelbene, and Yassine Bouazzi. "Unsteady magneto-hydro-dynamics flow of Jeffrey fluid through porous media with thermal radiation, Hall current and Soret effects." *Journal of Magnetism and Magnetic Materials* 582 (2023): 171033. https://doi.org/10.1016/j.jmmm.2023.171033

[15] Raghunath, Kodi. "Study of Heat and Mass Transfer of an Unsteady Magnetohydrodynamic (MHD) Nanofluid Flow Past a Vertical Porous Plate in the Presence of Chemical Reaction, Radiation and Soret Effects." *Journal of Nanofluids* 12, no. 3 (2023): 767-776. https://doi.org/10.1166/jon.2023.1923

[16] Raghunath, K., R. Mohana Ramana, V. Ramachandra Reddy, and M. Obulesu. "Diffusion Thermo and Chemical Reaction Effects on Magnetohydrodynamic Jeffrey Nanofluid Over an Inclined Vertical Plate in the Presence of Radiation Absorption and Constant Heat Source." *Journal of Nanofluids* 12, no. 1 (2023): 147-156. https://doi.org/10.1166/jon.2023.1923

[17] Maatoug, Samah, K. Hari Babu, V. V. L. Deepthi, Kaouther Ghachem, Kodi Raghunath, Charankumar Ganteda, and Sami Ullah Khan. "Variable chemical species and thermo-diffusion Darcy–Forchheimer squeezed flow of Jeffrey nanofluid in horizontal channel with viscous dissipation effects." *Journal of the Indian Chemical Society* 100, no. 1 (2023): 100831. https://doi.org/10.1016/j.jics.2022.100831

[18] Bafakeeh, Omar T., Kodi Raghunath, Farhan Ali, Muhammad Khalid, El Sayed Mohamed Tag-ElDin, Mowffaq Oreijah, Kamel Guedri, Nidhal Ben Khedher, and Muhammad Ijaz Khan. "Hall current and Soret effects on unsteady MHD rotating flow of second-grade fluid through porous media under the influences of thermal radiation and chemical reactions." *Catalysts* 12, no. 10 (2022): 1233. https://doi.org/10.3390/catal12101233

[19] Deepthi, V. V. L., Maha MA Lashin, N. Ravi Kumar, Kodi Raghunath, Farhan Ali, Mowffaq Oreijah, Kamel Guedri, El Sayed Mohamed Tag-ElDin, M. Ijaz Khan, and Ahmed M. Galal. "Recent development of heat and mass transport in the presence of Hall, ion slip and thermo diffusion in radiative second grade material: application of micromachines." *Micromachines* 13, no. 10 (2022): 1566. https://doi.org/10.3390/mi13101566

[20] Rani, Hari Ponnamma, and Chang Nyung Kim. "A numerical study of the Dufour and Soret effects on unsteady natural convection flow past an isothermal vertical cylinder." *Korean journal of chemical engineering* 26 (2009): 946-954. https://doi.org/10.1007/s11814-009-0158-y

[21] Pal, Dulal, and Hiranmoy Mondal. "Effects of Soret Dufour, chemical reaction and thermal radiation on MHD non-Darcy unsteady mixed convective heat and mass transfer over a stretching sheet." *Communications in Nonlinear Science and Numerical Simulation* 16, no. 4 (2011): 1942-1958. https://doi.org/10.1016/j.cnsns.2010.08.033

[22] Sharma, Bhupendra K., Kailash Yadav, Nidhish K. Mishra, and R. C. Chaudhary. "Soret and Dufour effects on unsteady MHD mixed convection flow past a radiative vertical porous plate embedded in a porous medium with chemical reaction." (2012). https://doi.org/10.4236/am.2012.37105

[23] Bestman, A. R. "Natural convection boundary layer with suction and mass transfer in a porous medium." *International journal of energy research* 14, no. 4 (1990): 389-396. https://doi.org/10.1002/er.4440140403

[24] Awad, Faiz G., Sandile Motsa, and Melusi Khumalo. "Heat and mass transfer in unsteady rotating fluid flow with binary chemical reaction and activation energy." *PloS one* 9, no. 9 (2014): e107622. https://doi.org/10.1371/journal.pone.0107622

[25] Dhlamini, Mlamuli, Peri K. Kameswaran, Precious Sibanda, Sandile Motsa, and Hiranmoy Mondal. "Activation energy and binary chemical reaction effects in mixed convective nanofluid flow with convective boundary conditions." *Journal of Computational Design and Engineering* 6, no. 2 (2019): 149-158. https://doi.org/10.1016/j.jcde.2018.07.002

[26] Anuradha, S., and K. Sasikala. "MHD free convective flow of a nanofluid over a permeable shrinking sheet with binary chemical reaction and activation energy." *International Journal of Engineering Science Invention* 7, no. 1 (2018): 22-30.

[27] Hamid, Aamir, and Masood Khan. "Impacts of binary chemical reaction with activation energy on unsteady flow of magneto-Williamson nanofluid." *Journal of Molecular Liquids* 262 (2018): 435-442. https://doi.org/10.1016/j.molliq.2018.04.095

[28] Huang, Chuo-Jeng. "Arrhenius Activation Energy Effect on Free Convection About a Permeable Horizontal Cylinder in Porous Media." *Transport in porous media* 128, no. 2 (2019): 723-740. https://doi.org/10.1007/s11242-019-01267-1

[29] Mustafa, M., Junaid Ahmad Khan, T. Hayat, and A. Alsaedi. "Buoyancy effects on the MHD nanofluid flow past a vertical surface with chemical reaction and activation energy." *International Journal of Heat and Mass Transfer* 108 (2017): 1340-1346. https://doi.org/10.1016/j.ijheatmasstransfer.2017.01.029

[30] Zaib, Aurang, Mohammad Mehdi Rashidi, Ali J. Chamkha, and Krishnendu Bhattacharyya. "Numerical solution of second law analysis for MHD Casson nanofluid past a wedge with activation energy and binary chemical reaction." *International Journal of Numerical Methods for Heat & Fluid Flow* 27, no. 12 (2017): 2816-2834. https://doi.org/10.1108/HFF-02-2017-0063

[31] Monica, M., J. Sucharitha, and C. H. Kishore. "Effects of exothermic chemical reaction with Arrhenius activation energy, non-uniform heat source/sink on MHD stagnation point flow of a Casson fluid over a nonlinear stretching sheet with variable fluid properties and slip conditions." *Journal of the Nigerian Mathematical Society* 36, no. 1 (2017): 163-190.

[32] Hayat, Tasawar, Ikram Ullah, Muhammad Waqas, and Ahmed Alsaedi. "Attributes of activation energy and exponential based heat source in flow of Carreau fluid with cross-diffusion effects." *Journal of Non-Equilibrium Thermodynamics* 44, no. 2 (2019): 203-213. https://doi.org/10.1515/jnet-2018-0049

[33] Shafique, Z., M. Mustafa, and A. Mushtaq. "Boundary layer flow of Maxwell fluid in rotating frame with binary chemical reaction and activation energy." *Results in Physics* 6 (2016): 627-633. https://doi.org/10.1016/j.rinp.2016.09.006

[34] Kodi, Raghunath, Charankumar Ganteda, Abhishek Dasore, M. Logesh Kumar, G. Laxmaiah, Mohd Abul Hasan, Saiful Islam, and Abdul Razak. "Influence of MHD mixed convection flow for maxwell nanofluid through a vertical cone with porous material in the existence of variable heat conductivity and diffusion." *Case Studies in Thermal Engineering* 44 (2023): 102875. https://doi.org/10.1016/j.csite.2023.102875